Boundary-Layer Meteorol (2008) 129:99–113
DOI 10.1007/s10546-008-9312-z

ORIGINAL PAPER

The Effect of Surface Heterogeneity on the Temperature–Humidity Correlation and the Relative Transport Efficiency

Arnold F. Moene · Dirk Schüttemeyer

Received: 10 July 2007 / Accepted: 25 August 2008 / Published online: 16 September 2008

Abstract We derive a conceptual model of the flow over heterogeneous terrain consisting of patches with contrasting Bowen ratios. Upward moving eddies are assumed to carry heterogeneous properties, whereas downward moving eddies carry homogeneous properties. This results in a decorrelation of temperature and humidity as the contrast between the patches increases. We show that this model is able to reproduce the relationship developed by Lamaud and Irvine (Boundary-Layer Meteorol. 120:87–109, 2006). Some details differ from their expression but are in accordance with data obtained over African savannah. We extend the conceptual model to a combination of any scalars, not necessarily linked through the surface energy balance (as is the case for temperature and humidity). To this end we introduce a new parameter that describes the surface heterogeneity in surface fluxes. The results of the current model can be used to predict the discrepancy between similarity relationships for different scalars over heterogeneous terrain.

Keywords Bkowen ratio · Surface heterogeneity · Surface layer similarity · θ–q-correlation · Variance method

1 Introduction

In the study of the turbulent atmospheric boundary layer (ABL) dimensional analysis is widely used. The rationale behind this use is that dimensional analysis often gives simpler relationships between properties of the flow than would be obtained by solving the governing equations (for mean quantities, variances, fluxes etc.). For flows in the lower part of the ABL the cornerstone of (the analysis of) experiments and modelling is Monin–Obukhov Similarity Theory (MOST). MOST relationships for mean gradients as well as variances and

A. F. Moene (✉) · D. Schüttemeyer
Wageningen University, Meteorology and Air Quality Group, PO Box 47, 6700 AA Wageningen, The Netherlands
e-mail: arnold.moene@wur.nl

D. Schüttemeyer
Meteorological Institute, University of Bonn, Bonn, Germany

other higher-order statistics (e.g. structure parameters) are widely used to determine surface fluxes from those statistics. Hence it is important to know under which conditions MOST is valid (Katul et al. 1995).

The simplicity of MOST is partly due to the strict conditions for its validity: stationarity, horizontal homogeneity and irrelevance of processes in the boundary layer (above the surface layer). These conditions limit the number of relevant variables. One of the consequences of MOST is that similarity relationships should be identical for all scalars, and the correlation between scalar fluctuations should be either $+1$ or -1 (Hill 1989).

In reality however, violations of one or more of the strict conditions for MOST are the rule rather than the exception: e.g. most natural surfaces are heterogeneous and conditions are often non-stationary, at least due to the diurnal cycle.

If not all conditions for MOST are met, decorrelation between scalars may occur. In two important cases this can be attributed to differences in source location, either horizontally or vertically. In the case of horizontal differences the scalar surface fluxes under consideration vary in an uncorrelated (or negatively correlated) way, as discussed by e.g. Beljaars et al. (1983), de Bruin et al. (1991), Roth and Oke (1995), Katul et al. (1995), Andreas et al. (1998), and recently Detto et al. (2008) (further referred to as DK08). Vertical differences occur if the relative importance of the surface flux and entrainment flux is different for both scalars: differences in entrainment regime (de Bruin et al. 1993; Michels and Jochum 1995; Jochum et al. 2004; Moene et al. 2006a). Other causes for decorrelation of scalars are the active role of temperature and humidity, modulations of the surface layer by the outer layer (and unsteadiness) and advective conditions (see Katul et al. (2008) for an extensive review of literature on this subject).

Here we will concentrate on the decorrelation between temperature and humidity caused by surface heterogeneity. More specifically, the similarity relationships for scalar standard deviations will be considered. For the standard deviation of a scalar s, σ_s, the general format of the similarity relationship is:

$$\frac{\sigma_s}{|s_*|} = f_s\left(\frac{z-d}{L}\right), \tag{1}$$

where $s_* \equiv -\overline{w's'}_0/u_*$, $u_* \equiv \sqrt{\tau/\rho}$, $L \equiv \left(\theta u_*^2\right)/(\kappa g \theta_{v*})$, τ is the surface shear stress, $\overline{w's'}_0$ is the surface flux of scalar x, d is the displacement height, ρ is the density of the air, θ_v is the virtual potential temperature, g is the gravitational acceleration and κ is the Von Karman constant. If all conditions of MOST are met, $f_s\left(\frac{z-d}{L}\right)$ should be identical for all scalars and the absolute value of the correlation coefficient between two scalars r and s (say θ and q) r_{rs} should be equal to unity (de Bruin et al. 1993; Hill 1989). If $|r_{\theta q}| = 1$, then $|r_{w\theta}| = |r_{wq}|$, and consequently, the following equality should hold:

$$\frac{\sigma_q}{q_*}\frac{\theta_*}{\sigma_\theta} = \frac{r_{w\theta}}{r_{wq}} \equiv \lambda = \pm 1, \tag{2}$$

where λ can be interpreted as a *relative* transport efficiency. Departure of the above expression from unity will occur simultaneously with a decorrelation of θ and q, i.e. $|r_{\theta q}| < 1$

Based on an extensive literature survey, Lamaud and Irvine (2006) (further referred to as LI06) deduced the following general trends:

- For wet conditions $\lambda = r_{\theta q}$,
- For dry conditions $\lambda = \frac{1}{r_{\theta q}}$.

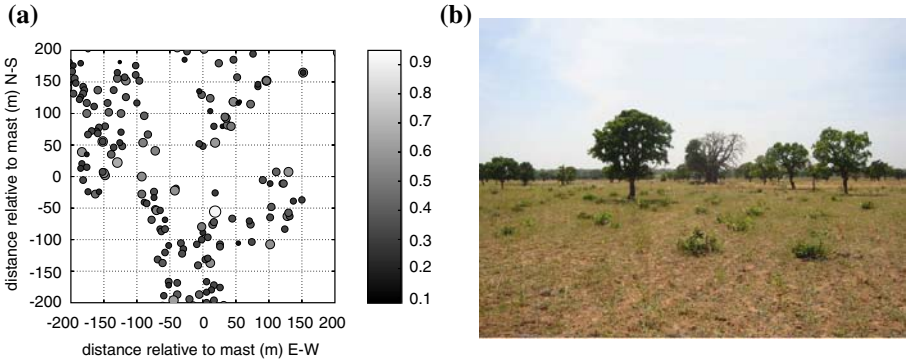

Fig. 1 Impression of the distribution of trees in the savannah around the eddy-covariance mast in Ghana. Left: tree density (the grey-scale indicates the stem diameter in m); right: taken just after the end of the rainy season (see Sect. 3 for details on time and location)

Furthermore they analysed a 3-month period of observations above ($z = 40\,\mathrm{m}$) and within ($z = 5\,\mathrm{m}$) a pine forest of 19 m height. The heterogeneity in their case stems both from the vertical structure within the canopy and the horizontal heterogeneity of the forest stand. From those data they derived an interpolation that both fills the gap between 'wet' and 'dry' (in terms of Bowen ratio, β) and better defines the limits of wet and dry conditions, viz.

$$\lambda = r_{\theta q}^{k} \quad \text{with} \begin{cases} k = 1 & \text{for } 0 < \beta \leq 0.1, \\ k = -1 - 2\log(\beta) & \text{for } 0.1 \leq \beta \leq 1, \\ k = -1 & \text{for } \beta \geq 1. \end{cases} \tag{3}$$

One of the consequences of this interpolation formula is that $\lambda = 1$ for $\beta = (\sqrt{(10)})^{-1} = 0.316$, irrespective of the value of the correlation between θ and q (i.e. $k = 0$). However, LI06 do not explain the origin of the Bowen ratio dependence of k.

In Sect. 2 we develop a conceptual model for a heterogeneous terrain with dry and wet patches, inspired by the situation for savannah vegetation in West Africa (see Figs. 1 and 2). For illustration purposes we use data from Schüttemeyer et al. (2006), which are discussed in Sect. 3. In Sect. 4 the model is used to explain the occurrence of decorrelation between temperature and humidity, and furthermore, the dependence of the exponent k on the Bowen ratio is investigated. Finally, the model is extended to a generic combination of scalars, not necessarily linked through the surface energy balance. Points of discussion are raised in Sect. 5, and the main conclusions are given in Sect. 6.

2 Theory

The model is inspired by the savannah landscape depicted in Fig. 1: a mixture of trees of about 5 m height that transpire throughout the wet *and* dry seasons (wet patches) and drying grass in between that becomes drier once the rain has ceased, and eventually disappears completely.

We will derive a simple model to show the dependence of $r_{\theta q}$ on the spatial heterogeneity of the Bowen ratio, and furthermore, the relationship between the mean Bowen ratio and the relative transport efficiency (λ) can be explained.

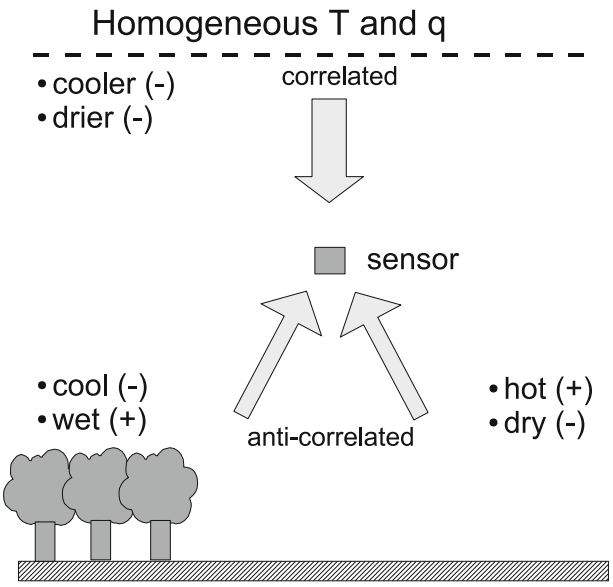

Fig. 2 Decorrelation of temperature and humidity due to inhomogeneity in vegetation cover

Figure 2 illustrates the central mechanism: vegetated and non-vegetated patches are mixed. The vegetated patches are relatively wet (high transpiration) and cool, whereas the bare soil patches are dry and hot. This implies that in rising eddies that originate randomly from either a bare soil patch or a vegetated patch temperature and humidity will be anti-correlated. If we assume that the sinking eddies originate from a level where the horizontal inhomogeneities have disappeared (i.e. above the blending height), temperature and humidity are positively correlated for downward motion.

2.1 Variance Budget

MOST for scalar variances implies an equilibrium between the production and dissipation of variance. Hence, deviations from MOST will be reflected in the fact that other terms in the variance budgets become non-negligible. Here we start from the scalar variance budget for stationary conditions, aligned with the mean wind and negligible mean vertical wind speed (see DK08):

$$\underbrace{\overline{u}\frac{\partial\overline{s's'}}{\partial x}}_{I} \approx \underbrace{-2\overline{u's'}\frac{\partial\overline{s}}{\partial x}}_{II}\underbrace{-2\overline{w's'}\frac{\partial\overline{s}}{\partial z}}_{III}\underbrace{-2\epsilon_s}_{IV}\underbrace{-TR}_{V} \tag{4}$$

where terms III and IV are the production and dissipation terms that balance for pure MOST conditions, term I is the advection of variance due to a mean horizontal gradient of variance, term II is an extra production term due to a horizontal gradient of mean scalar concentration, and term V (TR) is the turbulent transport term $\left(\text{in this case, } TR = \frac{\partial}{\partial x}\overline{u's's'} + \frac{\partial}{\partial z}\overline{w's's'}\right)$. In the present conceptual model (see Fig. 2) all three terms I, II and V may be relevant in producing extra variance. In a way similar to DK08, the terms I, II, III and V in the budget are estimated using relevant scales, as follows: $\frac{\partial}{\partial x} \sim 1/l_x$ where l_x is a characteristic length scale

of the horizontal inhomogeneity. Furthermore, $\frac{\partial}{\partial z} \sim 1/(\kappa z)$, vertical differences in $\overline{s} \sim s_*$ and in $\overline{s's'} \sim s_*^2$, whereas horizontal differences in $\overline{s} \sim \Delta s_*$ or $\overline{s's'} \sim (\Delta s_*)^2$. Here Δs_* is a measure of the horizontal contrast in surface fluxes (the latter scaling is not used by DK08). The turbulent fluxes are given by $\overline{w's'} = -u_* s_*$ and $\overline{u's'} \sim u_* s_*$ (see DK08). Furthermore, $\frac{\partial \overline{w's's'}}{\partial z} \sim 0$ (assuming a parameterization as in DK08 and negligible vertical flux divergence) and $\frac{\partial \overline{u's's'}}{\partial x} \sim \frac{u_*(\Delta s_*)^2}{l_x}$. Then the relative importance of the 'extra' terms I, II and V, relative to the production term III, can be estimated as $\frac{\kappa z}{l_x} \frac{\overline{u}}{u_*} \frac{(\Delta s_*)^2}{s_*^2}$ for term I, $\frac{\kappa z}{l_x} \frac{(\Delta s_*)}{s_*}$ for term II and $\frac{\kappa z}{l_x} \frac{(\Delta s_*)^2}{s_*^2}$ for term V. Hence it is clear that two conditions must be met before terms I, II and V can play a role in the production of 'extra' variance: the length scale of the heterogeneity should be of the same order (or less) as κz, and the contrast in surface fluxes between the different surfaces should at least be of the same order as the surface fluxes themselves.

2.2 Specification of the Patchy Surface

The surface is assumed to be covered with patches having Bowen ratios β_1 and β_2. The patches with β_1 cover a fraction α of the surface, those with β_2 a fraction $(1-\alpha)$. Furthermore, the magnitude of the inhomogeneity is expressed in the ratio $\gamma = \frac{\beta_1}{\beta_2}$. Note that we assume $\gamma > 0$, implying that the Bowen ratios for both patches have the same sign. This excludes situations in which one patch evaporates so strongly that the sensible heat flux is negative, whereas the other patch has positive sensible heat flux and evapotranspiration.

The mean Bowen ratio of the surface, $\overline{\beta}$ is:

$$\overline{\beta} = \frac{\alpha H_1 + (1-\alpha) H_2}{\alpha L_v E_1 + (1-\alpha) L_v E_2}, \tag{5}$$

where H_n and $L_v E_n$ are the surface sensible and latent heat fluxes of patch n, respectively. The available energy ($Q^* - G$, with Q^* being the net radiation, and G the soil heat flux) at the two patches may be different, which is expressed by $\epsilon = (Q^* - G)_1/(Q^* - G)_2$. One could expect that if patch 1 is vegetated and well-watered whereas patch 2 is dry with little or no vegetation, $\epsilon > 1$. In combination with $H_1 < H_2$ and $L_v E_1 > L_v E_2$ this leads to a situation where $|H_1 - H_2| < |L_v E_1 - L_v E_2|$, which is in line with the assumptions and observations of Andreas et al. (1998) and Katul et al. (1995,1999) that the sensible heat flux is less heterogeneous than the latent heat flux.

From this point one can derive for a given α, $\overline{\beta}$, γ and ϵ:

$$\beta_1 = \beta_2 \gamma, \tag{6}$$

$$\beta_2 = \left(\frac{-B \pm \sqrt{B^2 + 4AC}}{2A} \right)^{-1}, \tag{7}$$

with

$$A = \overline{\beta}\,(\alpha\epsilon + 1 - \alpha), \tag{8a}$$

$$B = \overline{\beta}\,(\alpha\epsilon + \gamma - \alpha\gamma) - \alpha\epsilon\gamma - 1 + \alpha, \tag{8b}$$

$$C = -\alpha\epsilon\gamma - \gamma + \alpha\gamma. \tag{8c}$$

Here we will only discuss the solution with a plus (+) in the expression for β_2. The solution with a minus (−) involves patches that both have a negative Bowen ratio, but with opposite directions of the fluxes (e.g. $H_1 > 0$ and $H_2 < 0$).

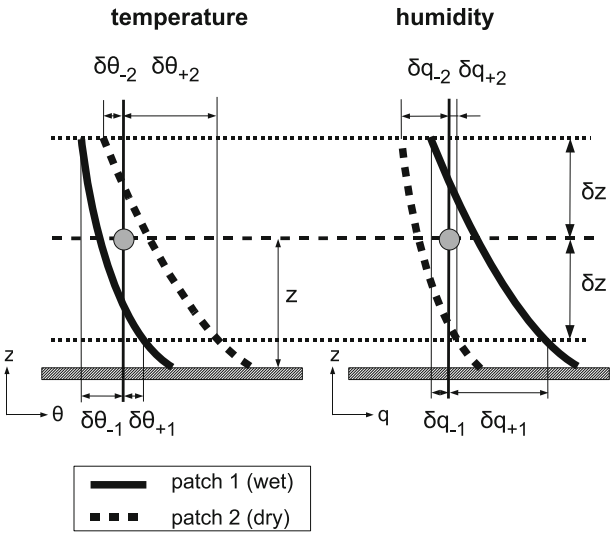

Fig. 3 Illustration of the origin of fluctuations in temperature and humidity as used in the model. The profiles of the two patches have been assumed to be equal arbitrarily at a height δz above the reference level

From the available energy for each patch (dependent on the average available energy and the ratio ϵ), in combination with the Bowen ratios β_1 and β_2, the sensible and latent heat fluxes for each of the patches can be computed. Those fluxes are needed to specify the turbulent scalar fluctuations in the next Subsection.

To reduce the number of variables, we now assume that the available energy for both patches is equal (i.e. $\epsilon = 1$). This assumption is not valid in general, given the effect of evapotranspiration on the surface temperature, differences in albedo between the patches and differences in soil heat flux.

2.3 Turbulent Fluctuations

Now that the surface conditions have been defined, the effect of these conditions on turbulent scalar fluctuations need to be considered. The model is based on a very simplistic view of surface-layer turbulence (see Fig. 3).

- Turbulent fluctuations of a scalar are produced by parcels of air that carry conserved properties from a certain level to the observation level. These parcels are assumed to come from a fixed distance above and below the observation level (distance equal for downward and upward motions);
- The parcels originate from a location above one of the patches and are displaced horizontally either by the mean wind or by horizontal velocity fluctuations. Both processes could loosely be interpreted as being representative of terms I and II in the variance budget, respectively (Eq. 4).
- The values of the conserved quantities at these originating levels are assumed to be described by standard flux–gradient relationships for the *mean* gradients.

The net effect is that (for positive fluxes) downward moving parcels generate negative fluctuations in both scalars that are better correlated than the positive fluctuations of the upward moving parcels. The net effect is that fluctuations of both scalars decorrelate, depending on

the relative magnitude of vertical differences, and (horizontal) differences in scalars between the patches (i.e. $s_*/(\Delta s_*)$).

This leads to the following expressions for scalar fluctuations related to downward motion (δs_-) and upward motion (δs_{+i}):

$$\delta s_{-i} = s_{*i}\, g(z - \delta z, z, L) - \overline{\delta s}, \tag{9}$$

$$\delta s_{+i} = s_{*i}\, g(z + \delta z, z, L) - \overline{\delta s}, \tag{10}$$

with $g(z_1, z_2, L) = \ln(z_1/z_2) - \Psi_s(z_1/L) + \Psi_s(z_2/L)$. The index i indicates the originating patch, Ψ_x is the integrated flux–gradient relationship for scalars (Paulson 1970) consistent with the flux–gradient relationships of Dyer and Hicks (1970) used below, δz is the vertical distance over which the parcels have travelled and $\overline{\delta s}$ is the (weighted) mean at height z of the fluctuations from the two patches, taking both rising and sinking parcels into account (the exact expression for $\overline{\delta s}$ is given later, see Eq. 12). The subtraction of $\overline{\delta s}$ is needed to correct for the fact that the scalar profiles for both patches do not necessarily coincide at height z.

To determine L the mean value of θ_{v*} is used. The atmospheric stability is assumed to be not influenced by the patch under consideration, so the same value of L is used for the rising and sinking parcels from both patches.

For the specification of the distance from where the parcels originate (δz) use is made of the similarity relationships for the scalar standard deviation σ_s and the scalar gradient $\partial\overline{s}/\partial z$. Here, δz is that height interval that a parcel should travel along a constant vertical gradient to explain a given standard deviation. This leads to the following expression for δz:

$$\delta z = \frac{f_s\left(\frac{z}{L}\right)}{f_s(0)} \frac{\kappa z}{\phi_s\left(\frac{z}{L}\right)}, \tag{11}$$

where $f_s\left(\frac{z}{L}\right) = \sigma_s/s_*$ (see Eq. 1) and $\phi_s\left(\frac{z}{L}\right) = (\kappa z/s_*)\,\partial\overline{s}/\partial z$, where the functions of Dyer and Hicks (1970) are used. This expression gives a neutral mixing length of κz. It should be noted that the outcomes of the model appear to be rather insensitive to the exact formulation for δz.

In order to determine the scalar variances, covariance and the kinematic flux from δs and δr, a few extra quantities need to be defined:

- A fixed correlation coefficient between scalar fluctuations and vertical wind speed fluctuations ($\widehat{r}_{ws}$) is assumed independent of the direction of the movement (up or down), or the originating patch (1 or 2). Although the exact value of $\widehat{r}_{ws}$ is not relevant, it can be deduced from the similarity relationships of σ_w and σ_θ that $r_{w\theta}$ is approximately 0.25–0.55.
- An undefined value for the vertical wind speed variance σ_w^2 is assumed.

A fraction α of the parcels originates from patches with β_1 and $(1-\alpha)$ originates from patches with β_2. With these assumptions, estimates can be made for the mean of the fluctuations (needed in Eqs. 9 and 10), variances ($\overline{s's'}$), scalar covariances ($\overline{s'r'}$) and scalar-vertical wind covariances ($\overline{w's'}$):

$$\overline{\delta s} = \left(\alpha\delta s'_{-1} + (1-\alpha)\delta s'_{-2}\right) + \left(\alpha\delta s'_{+1} + (1-\alpha)\delta s'_{+2}\right), \tag{12}$$

$$\overline{s's'} = \left(\alpha\delta s^2_{-1} + (1-\alpha)\delta s^2_{-2}\right) + \left(\alpha\delta s^2_{+1} + (1-\alpha)\delta s^2_{+2}\right), \tag{13}$$

$$\overline{s'r'} = (\alpha\delta s_{-1}\delta r_{-1} + (1-\alpha)\delta s_{-2}\delta r_{-2}) + (\alpha\delta s_{+1}\delta r_{+1} + (1-\alpha)\delta s_{+2}\delta r_{+2}), \quad (14)$$

$$\overline{w's'} \equiv \sigma_w \widehat{r}_{ws} \left(-(\alpha\delta s_{-1} + (1-\alpha)\delta s_{-2}) + (\alpha\delta s_{+1} + (1-\alpha)\delta s_{+2})\right), \quad (15)$$

where s'_{-i} and s'_{+i} are the fluctuations as given in Eqs. (9) and (10), but without the mean substracted. From Eqs. 13 and 14 the correlation coefficient can be determined, and furthermore, from 13 and 15 the transport efficiency (r_{ws}) can be determined.

The magnitude of the fluctuations δx depend on s_* and the mixing length δz. The stability z/L, needed to determine δz is an internal variable. If a range of conditions with varying $\overline{\beta}$ (and thus varying z/L) needs to to be compared, the fact that z/L depends on $\overline{\beta}$ would create extra variability. Therefore, we define an extra external dimensionless number, z/L_{AE}, where L_{AE} is an Obukhov length with the buoyancy flux replaced by the available energy: $L_{AE} \equiv \left(\theta u_*^3 \rho c_p\right) / \left(\kappa g (Q^* - G)\right)$. From L_{AE} and the mean Bowen ratio $\overline{\beta}$ the actual L is deduced that is used to compute δz.

3 Observations

For illustration purposes, observations gathered at a savannah site in Ghana are used. These were gathered between November 4, 2002 and December 10, 2002 near Tamale, Ghana (9°29′ N, 0°55′ W). Eddy-covariance equipment was installed at 10-m height, consisting of a CSAT-3D (Campbell Scientific) sonic anemometer and an IrGA 7500 (LiCor) infrared gas analyzer (water vapour and CO_2). From the raw data half-hourly mean fluxes have been computed. For details on the data processing, see Schüttemeyer et al. (2006) and van Dijk et al. (2004).

Within 1 month the evapotranspiration decreased dramatically: at the start grass, bushes and trees transpired nearly unrestricted, whereas toward the end of the period the grass died, and only the trees were able to transpire without restrictions. The midday Bowen ratio of the terrain increased from 0.5 to 3 over 1 month (Moene et al. 2006b). Figure 1 gives an impression of the tree density around the eddy-covariance mast. The mean density is of the order of 17 trees per hectare (or a mean distance between the trees of 25 m) but the trees are very unevenly spread, especially in the vicinity of the flux tower.

4 Consequences of the Model

4.1 Temperature-Humidity Correlation

Figure 4 shows the resulting correlation coefficients for two distributions of ‘dry’ and ‘wet’ patches, viz. $\alpha = 0.5$ and $\alpha = 0.15$, the latter distribution being inspired by the Ghanean savannah vegetation. The first thing to note is that with an increasing Bowen ratio contrast between the patches, $r_{\theta q}$ decreases, due to the fact that the contrast between fluctuations originating from different patches (δs_{+1} and δs_{+2}) becomes large relative to the fluctuations related to the vertical scalar gradient. Furthermore, for $\alpha = 0.5$, $r_{\theta q}$ has a minimum for a mean Bowen ratio equal to one. This combination of α and $\overline{\beta}$ gives the largest contrast between the surface values of θ and q for the two patches, and consequently $\sigma_\theta \sigma_q$ is at its

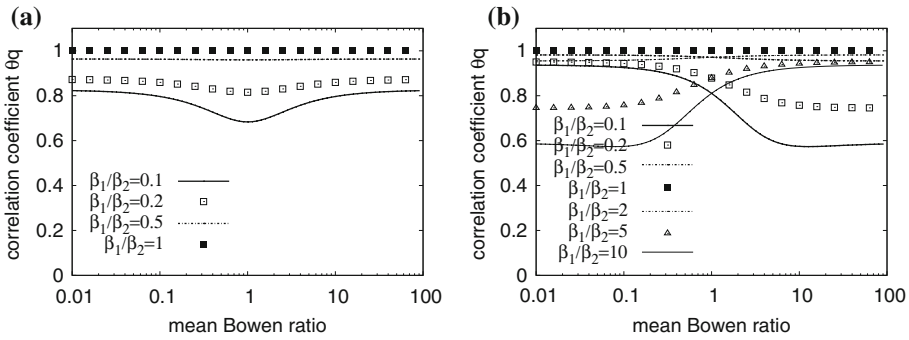

Fig. 4 Dependence of the θq correlation coefficient on the Bowen ratios of the individual patches and the mean Bowen ratio. (**a**) Fraction with β_1 equals that with β_2. The lines for a given ratio β_1/β_2 coincide with those with a ratio that is the inverse; (**b**) fraction with β_1 is 15%

maximum, thus reducing $r_{\theta q}$. For other values of α the maxima of the $\theta - q$ covariance and $\sigma_\theta \sigma_q$ (both not shown) are also located near $\overline{\beta} = 1$, but with decreasing α (smaller 'wet' patches with β_1) the maximum in $\overline{\theta' q'}$ becomes more pronounced and shifts to lower $\overline{\beta}$; in contrast the maximum in $\sigma_\theta \sigma_q$ decreases and shifts to higher $\overline{\beta}$. The net effect is that for smaller α the minimum in $r_{\theta q}$ shifts to higher $\overline{\beta}$ for $\beta_1/\beta_2 < 1$ (and lower $\overline{\beta}$ for $\beta_1/\beta_2 > 1$). To summarize: the smaller the wet patches, the drier the mean conditions need to be to obtain maximum decorrelation.

4.2 Relative Transport Efficiency for Moisture and Heat

Figure 5 shows the transport efficiencies for temperature and humidity ($r_{w\theta}$ and r_{wq}) for a range of mean Bowen ratios and ratios of the Bowen ratios of the individual patches (β_1/β_2). The first thing to note is that the correlation coefficients have been scaled with the correlation coefficient for homogeneous conditions, $\widehat{r}_{ws}$. Here $\widehat{r}_{ws}$ has been taken from the model itself (setting β_1/β_2 to one). This normalization with $\widehat{r}_{ws}$ masks the fact that r_{ws} depends on stability due to the fact that $f_s\left(\frac{z}{L}\right) f_w\left(\frac{z}{L}\right)$ is a function of stability: with increasing instability $\widehat{r}_{ws}$ increases. In the present model the increase in instability is linked to an increase in the mean Bowen ratio: although z/L_{AE} is fixed at -0.2, the actual stability changes to more unstable conditions with increasing Bowen ratio.

For $r_{w\theta}$ the largest deviations from unity occur at low Bowen ratios, whereas for r_{wq} the deviations occur for high Bowen ratios. However, these deviations only occur for relatively large contrasts between the patches: β_1/β_2 or $\beta_2/\beta_1 = 5$ and larger.

Figure 6a shows the relative transport efficiency λ as a function of the mean Bowen ratio. The first striking feature is that $\lambda = 1$ at $\overline{\beta} = 1$ for all cases, due to the fact that at $\overline{\beta} = 1$ the smaller temperature fluctuations originating from the wet patch are exactly compensated by the larger fluctuations from the dry patch (and the reverse for humidity). The net effect is that temperature and humidity behave identically, despite the fact that $r_{\theta q}$ is unequal to 1 (see Fig. 4).

In accordance with the findings for $r_{w\theta}$ and r_{wq}, relatively large contrasts in the Bowen ratios of the patches are needed to produce a significant deviation of λ from 1. For example, for λ to deviate from one by more than 10%, the mean Bowen ratio needs to be larger than 3, or less than 0.2, in combination with a contrast between the patches of γ or $1/\gamma$ larger

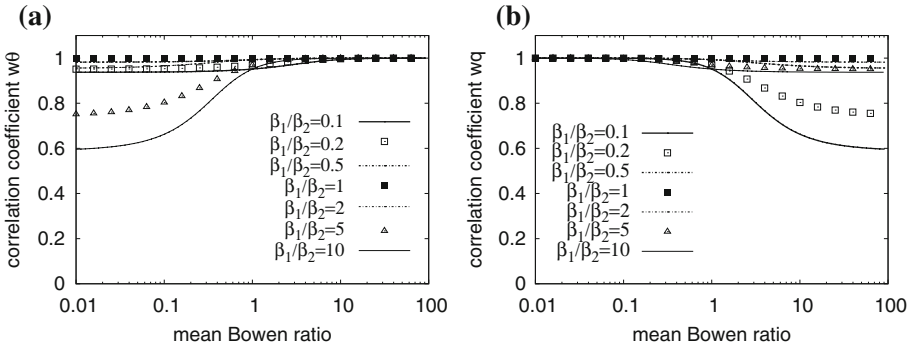

Fig. 5 Dependence of the correlation coefficient r_{ws} on Bowen ratios of the individual patches and the mean Bowen ratio. The patches with Bowen ratio β_1 occupy 15% of the surface. (**a**) $w\theta$ correlation coefficient; (**b**) wq correlation coefficient. In both cases the correlation coefficient for homogeneous conditions ($\widehat{r}_{ws}$) has not been taken into account: the depicted correlation coefficients are in fact $r_{ws}/\widehat{r}_{ws}$

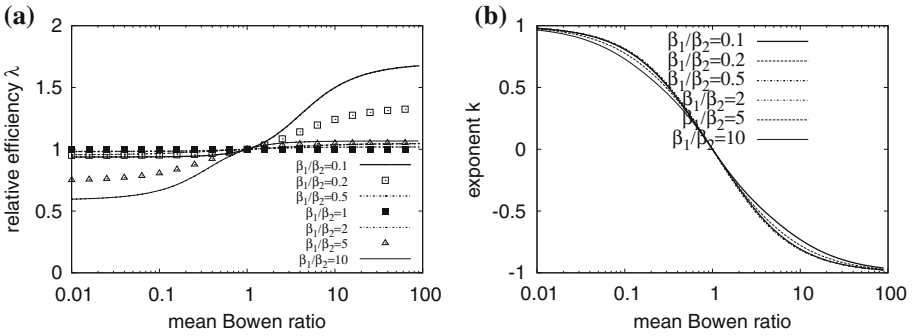

Fig. 6 (**a**) relative transport efficiency λ (for legend of lines and symbols, see Fig. 5); (**b**) the exponent k in the expression $\lambda = r_{\theta q}^{k}$. For both plots the surface fraction of β_1 is 0.15, the stability as expressed by z/L_{AE} is -0.2 and the fraction of parcels moving upward equals that of parcels moving down

than 5. In fact, λ is less than one for surfaces that are well-watered in the mean, and is larger than one for dry surfaces. The values of λ shown in Fig. 6 are much smaller than λ equal to 1.28 observed by Andreas et al. (1998) for Bowen ratios between 1 and 2. If our model is a good representation of reality, the large value for λ observed by Andreas et al. (1998) could not be due to surface heterogeneity only. For the data presented by LI06 a similar argument holds: for Bowen ratios well above unity they found values for λ of 1.5 and higher, which in the present model would require extreme differences between the patches.

One of the important results of LI06 is the expression that describes the way in which the relationship between λ and $r_{\theta q}$ depends on the Bowen ratio. Therefore, we investigate the Bowen ratio dependence of the exponent k in Eq. 3 as resulting from our conceptual model. The result is shown in Fig. 6b. The model predicts the limiting values of $k = 1$, $k = 0$ and $k = -1$ for low, intermediate and high Bowen ratios, respectively. The shape of the curve is similar to the Bowen ratio dependence of k as shown in Fig. 7 in LI06. It is striking that the shape of the curves is nearly insensitive to the contrast between the patches (as expressed by β_1/β_2).

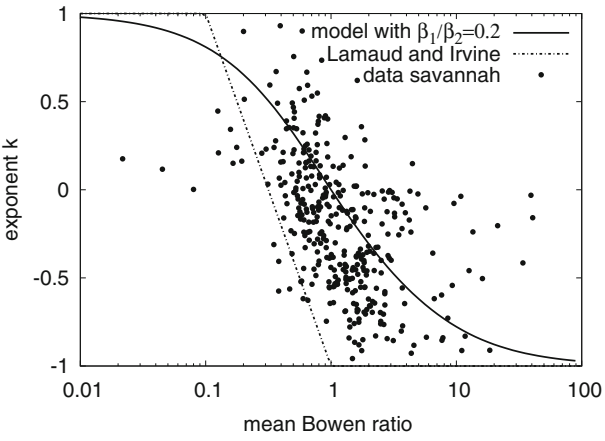

Fig. 7 The exponent k in the expression $|\lambda| = |r_{\theta q}|^k$ as obtained from our model with $\beta_1/\beta_2 = 0.2$, α is 0.15, the stability as expressed by z/L_{AE} is -0.2. Also shown is the parametrization of LI06, and k as obtained from the savannah data (which were filtered with the condition that the measured Bowen ratio had a statistical error of less than 20%)

To enable a better comparison between the current model, the parametrization of LI06 and our own data, Fig. 7 shows these three together. There are several main differences: the Bowen ratio for which $k = 0$ is exactly one for the current model, whereas it is 0.3 for the parametrization of LI06. On the other hand the slope of k versus $\log(\beta)$ of LI06 at intermediate Bowen ratios is similar to that in our data, whereas our model shows a smaller slope. Finally, the data (and the parametrization) of LI06 reach a value of -1 and 1 for $\beta = 0.1$ and $\beta = 1$ respectively, whereas Fig. 6b shows a more smooth transition. Regarding the Bowen ratio for which $k = 0$, it appears from our own data that the value cited by LI06 (0.31) is not universal: the present data suggest a value around one, in accordance with the current model (see Sect. 5).

4.3 Extension to Other Scalar Combinations

For combinations of scalars other than temperature and humidity, there is no logical equivalent for the mean Bowen ratio. However, in the context of the present model $\overline{\beta}$ is only used as an indicator of the relative importance of vertical and horizontal differences in temperature and humidity. At low $\overline{\beta}$ horizontal differences in temperature might dominate over vertical differences, leading to low values of $r_{w\theta}$, whereas for high $\overline{\beta}$ horizontal differences in humidity might be larger than vertical differences leading to a low transport efficiency for humidity, r_{wq}.

For the combination of temperature and humidity, the mean Bowen ratio is the determining factor for the scalar decorrelation because the relative importance of the vertical and the horizontal differences for both scalars is linked through the Bowen ratio. In order to make the transition to a generic combination of scalars we are forced to explicitly include information on the magnitude of the horizontal contrast. Here we propose the following generic measure of scalar surface heterogeneity (as a replacement for the mean Bowen ratio):

$$B = -\frac{F_{r1} - F_{r2}}{\overline{F}_r} \frac{\overline{F}_s}{F_{s1} - F_{s2}} = -\frac{\Delta r_*}{r_*} \frac{s_*}{\Delta s_*}, \tag{16}$$

where $\overline{F}_s$ and $\overline{F}_r$ are the areally-averaged surface fluxes of scalar s and r, and F_{s1}, F_{s2}, F_{r1} and F_{r2} are the fluxes for the individual patches. Note that the ratio $(\Delta s_*)/s_*$ that was introduced for the analysis of the variance budget appears here again.

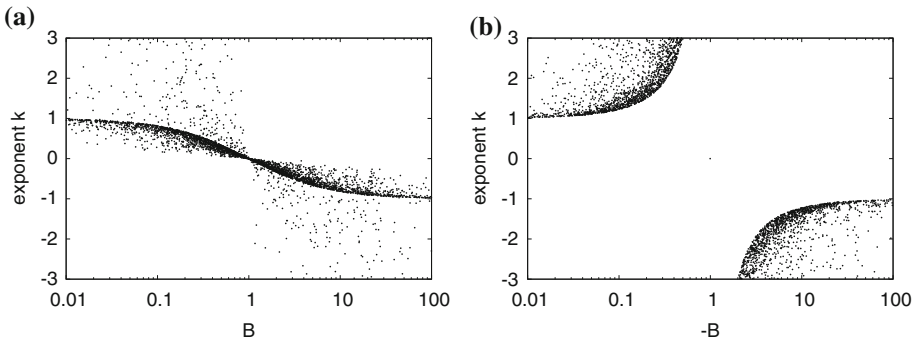

Fig. 8 The exponent k in the expression $\lambda_{sr} = r_{sr}^{k}$. For both plots the surface fraction of patch 1 is 0.15, the stability as expressed by z/L_{AE} is -0.2 and the fraction of parcels moving upward equals that of parcels moving down. (**a**) For $B > 0$, and (**b**) for $B < 0$, with $-B$ on the abscissa

For the combination of temperature ($s = \theta$) and humidity ($r = q$), with the surface fluxes of s and r being anti-correlated between the patches, B appears to be identical to $\overline{\beta}$ (provided that the available energy is equal for both patches). With $\lambda_{sr} \equiv r_{ws}/r_{wr}$, $|\lambda_{sr}| = |r_{sr}|^{k_{sr}}$ and replacing $\overline{\beta}$ by B, the dependence of k on surface conditions can be extended to any combination of scalars. In order to illustrate the utility of B defined above, we have generated a dataset of 10,000 sets of random surface fluxes for both s and r for each of the patches, and computed B and k_{sr} for each combination. In Fig. 8a the exponent k_{sr} is shown for positive values of B, which is a situation similar to the combination of temperature and humidity when the available energy is identical for the patches. Figure 8b shows the cases with $B < 0$, implying a positive correlation between the fluxes of s and r. The majority of points is located on relatively well-defined lines, where the curve for $B > 0$ is similar to the line in Fig. 7. The line again passes through a single point for $B = 1$ and $\lambda_{sr} = 1$, which is due to the fact that at $B = 1$ the surface fluxes of the two scalars are perfectly anti-correlated and the situation is similar to the situation for temperature and humidity at $\overline{\beta} = 1$: both r_{ws} and r_{wr} are smaller than one but equal, resulting in $\lambda_{sr} = 1$. The singularity at $B = -1$ is due to the fact that r_{sr} equals 1 at $B = -1$, whereas λ_{sr} can have a range of values, implying that k_{sr} can assume a large range of values.

5 Discussion

The present model does not take into account the arrangement of the patches, or the scale of individual patches. But from the analysis of the variance budget in Sect. 2.1 it is clear that the scale of the heterogeneities should be at most of the order of the observation height in order to have a noticeable effect on the variance budget. However, not only is the scale of the heterogeneities important, but also the relative contrast between the patches ($(\Delta s_*)/s_*$) plays an important role in determining the extent to which MOST conditions are violated.

In fact, it has been tacitly assumed that the downward moving parcels, originating at $z + \delta z$ (see Fig. 3), roughly originate from the level where temperature and humidity become more or less horizontally homogeneous (the scalar blending height, similar to the momentum blending height (Wieringa 1986)). If we make this assumption explicit, the model *does* take into account the scale of the heterogeneity, since the blending height will depend, among other things, on the scale of the heterogeneity.

However, the level where horizontal differences disappear does also depend on the magnitude of horizontal variations that *is* permitted (i.e. the extent to which horizontal differences have disappeared). If that permitted variation is determined relative to the vertical variation of the scalar under consideration, the blending heights for temperature and humidity may be different. For dry conditions (high β) the blending height for temperature is located lower than that of humidity, and for wet conditions (low β) the reverse holds. This implies that for dry conditions the temperature signal behaves as if it is related to a horizontally homogeneous surface (and the same holds for humidity for wet conditions). This may be the basis for the remark of Andreas et al. (1998) that for their observations the heat sources are (more) uniform than the moisture sources. This also explains that for temperature they found similarity relationships that are identical to those for a homogeneous surface.

One of the important differences between our model and the results of LI06 is the value of the Bowen ratio for which $k = 0$ ($\beta = 1$ in our model and $\beta = 0.31$ in LI06). A possible explanation for this discrepancy may be the fact that we assumed $\epsilon = 1$ (i.e. equal available energy for both patches). It turns out (not shown here) that a combination of patches where the wet patches have larger available energy than the dry patches ($\beta_1/\beta_2 < 1$ and $\epsilon > 1$) results in a downward shift of the k versus β line in Fig. 6b, and as a consequence the point where $k = 0$ shifts to lower values of $\overline{\beta}$. It should be noted that in the current model the difference in available energy between the patches should be considerable: ϵ should be of the order of 2, also resulting in a shift of the limiting values of k to 0.5 (small β) and -2.5 (large β).

Another remark to be made is that the present conceptual model does not take into account other violations of the assumptions underlying MOST, in particular the effects of entrainment. However, a model similar to the present one could be constructed to study the impact of entrainment effects. In that case, the fluctuations of a scalar should be considered as being the result of the superposition of fluctuations related to two processes. Fluctuations of the first kind are produced by vertical motion in a mean field with a vertical gradient (similar as in Fig. 3). Fluctuations of the second kind are related to large scale motions through the entire boundary layer, which become mostly horizontal in the surface layer (see e.g. McNaughton 2004). These fluctuations are thus *not* correlated to the vertical velocity. For a boundary layer where the entrainment ratio of moisture differs considerably from that of temperature, this leads to relatively large fluctuations of the second kind for moisture, whereas the temperature fluctuations are hardly affected. The variance of a scalar can then be considered to be the sum of the variance due to fluctuations of the first kind and fluctuations of the second kind. The relative transport efficiency λ is then dependent on the relative magnitude of the entrainment ratios of both scalars (compare this to the dependence on the Bowen ratio in the present model).

Finally, the model is purely one-dimensional in the sense that no interaction between the eddies originating from different patches is allowed for. In reality enhanced evaporation may occur when dry air from a dry patch is advected over a wet patch (see e.g. Diaz-Espejo et al. 2005).

6 Conclusions

It was shown by LI06 that the relative transport efficiency of heat and water vapour (λ) depends on the Bowen ratio and the temperature–humidity correlation. A simple conceptual model of a heterogeneous surface, consisting of two types of patches with contrasting Bowen ratios, can be used to explain this behaviour of λ. For dry conditions the horizontal contrast in humidity between the patches is much larger than the vertical contrast between the surface

and atmosphere. This results in a decrease in the correlation between vertical wind speed and humidity, and consequently in an increase in the ratio $r_{w\theta}/r_{wq} \equiv \lambda$. For wet conditions the reverse argument holds.

The model predicts the correct limits for the exponent k in $\lambda = r_{\theta q}^{k}$, but the Bowen ratio for which $k = 0$ is somewhat higher than the value quoted by LI06 (1 versus 0.31) but more in agreement with the observations of Schüttemeyer et al. (2006). In order to extend the application of the model to other combinations of scalars, a new generic measure of scalar surface heterogeneity (as a replacement of the mean Bowen ratio) has been introduced. Using synthetic data, it was shown that this new measure of surface heterogeneity is able to explain the variation in the exponent k_{sr} in $\lambda_{sr} = r_{sr}^{k_{sr}}$.

The results of the current model can be used to predict the discrepancy between similarity relationships for different scalars over heterogeneous terrain. This is particularly relevant if the variance method is used to derive fluxes. The surface heterogeneity may be related to the properties of natural vegetation (as for a savanna vegetation), or may be due to man-made heterogeneity (e.g. cropping patterns, urban areas).

Acknowledgements This work has been supported financially in part by the German Federal Ministry of Education and Research, Germany in the framework of the GLOWA-Volta project. Further financial support was provided in the framework of the project 'Integrated observations and modelling of Greenhouse Gas budgets at the national level in the Netherlands', part of the program 'Climate changes Spatial Planning'. The authors would like to thank Raymond Kasei, Ronald Groen and Gabriel Akotia for assistance in the field in Ghana. Furthermore, we would like to thank Henk de Bruin for his inspiring comments. Finally, we thank two anonymous reviewers for their very constructive comments.

References

Andreas EL, Hill RJ, Gosz JR, Moore DI, Otto WD, Sarma AD (1998) Statistics of surface-Layer turbulence over terrain with metre-scale heterogeneity. Boundary-Layer Meteorol 86:379–408

Beljaars ACM, Schotanus P, Nieuwstadt FTM (1983) Surface layer similarity under nonuniform fetch conditions. J Clim Appl Meteorol 22:800–1810

de Bruin HAR, Bink NJ, Kroon LJM (1991) Fluxes in the surface layer under advective conditions. In: Schmugge TJ, André JC (eds,) Land surface evaporation. Spinger-Verlag, Berling, pp 157–171.

de Bruin HAR, Kohsiek W, van den Hurk BJJM (1993) A verification of some methods to determine the fluxes of momentum, sensible heat, and water vapour using standard deviation and structure parameter of scalar meteorological quantities. Boundary-Layer Meteorol 63:231–257

Detto M, Katul G, Mancini M, Montaldo N, Albertson JD (2008) Surface heterogeneity and its signature in higher-order scalar similarity relationships. Agric For Meteorol 148:902–916

Diaz-Espejo A, Verhoef A, Knight R (2005) Illustration of micro-scale advection using grid-pattern mini-lysimeters. Agric For Meteorol 129(1/2):39–52

Dyer AJ, Hicks BB (1970) Flux–gradient relationships in the constant flux layer. Quart J R Meteorol Soc 96:715–721

Hill RJ (1989) Implications of Monin–Obukhov similarity theory for scalar quantities. J Atmos Sci 46:2236–2251

Jochum AM, Camino ER, De Bruin HAR, Holtslag AAM (2004) Performance of HIRLAM in a semiarid heterogeneous region: evaluation of the land surface and boundary layer description using EFEDA observations. Mon Wea Rev 132:2745–2760

Katul G, Goltz SM, Hsieh C-I, Cheng Y, Mowry F, Sigmon J (1995) Estimation of surface heat and momentum fluxes using the flux-variance method above uniform and non-uniform terrain. Boundary-Layer Meteorol 74:237–260

Katul G, Hsieh CI, Bowling D, Clark K, Shurpali N, Turnipseed A, Albertson J, Tu K, Hollinger D, Evans B et al (1999) Spatial variability of turbulent fluxes in the roughness sublayer of an even-aged pine forest. Boundary-Layer Meteorol 93(1):1–28

Katul GG, Sempreviva AM, Cava D (2008) The temperature–humidity covariance in the marine surface layer: a one-dimensional analytical model. Boundary-Layer Meteorol 126(2):263–278

Lamaud E, Irvine M (2006) Temperature-humidity dissimilarity and heat-to-water vapour transport efficiency above and within apine forest canopy: the role of the Bowen ratio. Boundary-Layer Meteorol 120(1): 87–109

McNaughton KG (2004) Turbulence structure of the unstable atmospheric surface layer and transition to the outer layer. Boundary-Layer Meteorol 112(2):199–221

Michels BI, Jochum AM (1995) Heat and moisture flux profiles in a region with inhomogeneous surface evaporation. J Hydrol 166:383–407

Moene AF, Michels BI, Holtslag AAM (2006a) Scaling variances of scalars in a convective boundary layer under different entrainment regimes. Boundary-Layer Meteorol 120:257–274

Moene AF, Schüttemeyer D, Hartogensis OK (2006b) Scalar similarity functions: the influence of surface heterogeneity and entrainment. In: 17th symposium on boundary layers and turbulence, 22–25 May 2006, San Diego, California. American Meteorological Society, Boston, p 5.1

Paulson CA (1970) The Mathematical Representation of Wind Speed and Temperature Profiles in the Unstable Atmospheric-Surface Layer. J Appl Meteorol 9:857–861

Roth M, Oke TR (1995) Relative efficiencies of turbulent transfer of heat, mass, and momentum over a patchy urban surface. J Atmos Sci 52:1863–1874

Schüttemeyer D, Moene AF, Holtslag AAM, de Bruin HAR, van de Giesen N (2006) Surface fluxes and characteristics of drying semi-arid terrain in West Africa. Boundary-Layer Meteorol 118:583–612

van Dijk A, Moene AF, de Bruin HAR (2004) The principles of surface flux physics: theory, practice and description of the {ECPACK} library. Internal report 2004/1. Wageningen University, Meteorology and Air Quality Group

Wieringa J (1986) Roughness-dependent geographical interpolation of surface wind speed averages. Quart J Roy Meteorol Soc 112:867–889